The Journal of Physiology, 31 January (2018)

DOI: https://doi.org/10.1113/JP275030

Role of fetal nutrient restriction and postnatal catch up growth on structural and mechanical alterations of rat aorta

Running title: Fetal undernutrition and aorta mechanical properties

[1]Perla Y Gutiérrez-Arzapalo, PhD; [1]Pilar Rodríguez-Rodríguez, PhD; [1]David Ramiro-Cortijo, MSc; [1]Ángel L López de Pablo, PhD; [2]Mª Rosario López-Giménez, PhD; [1]Luis Condezo-Hoyos, PhD; [3]Stephen E Greenwald, PhD; [1]Mª Carmen González, PhD and [1]*Silvia M Arribas, PhD.

[1]Department of Physiology and [2]Department of Preventive Medicine, Public Health and Microbiology, Faculty of Medicine, Universidad Autónoma de Madrid (Spain).

[2]Blizard Institute, Barts & The London School of Medicine & Dentistry, Queen Mary University of London (United Kingdom).

***Corresponding author:**
Dr. Silvia M Arribas
Department of Physiology
Faculty of Medicine
Universidad Autónoma de Madrid
C/ Arzobispo Morcillo 2, Madrid 28029, Spain
E-mail: silvia.arribas@uam.es
Tel: (+34) 91 497 6995
FAX: (+34) 914975478

Key words: Collagen; Elastin; Fetal Programming; Hypertension; IUGR; Vascular mechanics; Sexual dimorphism.

The Table of Contents category: Cardiovascular.

Key point summary

- Intrauterine growth restriction (IUGR), induced by maternal undernutrition leads to impaired aortic development. This is followed by hypertrophic remodeling associated with accelerated growth during lactation.
- Fetal nutrient restriction is associated with increased aortic compliance at birth and at weaning, but not in adult animals. This mechanical alteration may be related to a decreased perinatal collagen deposition.
- Aortic elastin scaffolds purified from young male and female IUGR animals also exhibit increased compliance, only maintained in adult IUGR females. These mechanical alterations may be related to differences in elastin deposition and remodeling.
- Fetal undernutrition induces similar aortic structural and mechanical alterations in young male and female rats.
- Our data argue against an early mechanical cause for the sex differences in hypertension development induced by maternal undernutrition. However, the larger compliance of elastin in adult IUGR females may contribute to the maintenance of a normal blood pressure levels.

Abstract. Fetal undernutrition programs hypertension development, males being more susceptible. Deficient fetal elastogenesis and vascular growth is a possible mechanism. We investigated the role of aortic mechanical alterations in a rat model of hypertension programming, evaluating changes at birth, weaning and adulthood. Dams were fed *ad-libitum* (Control) or 50% of control intake during the second half of gestation (maternal undernutrition, MUN). 3-day, 21-day and 6-month old offspring were studied. Blood pressure was evaluated *in vivo*. In the thoracic aorta we assessed gross structure, mechanical properties (intact and purified elastin), collagen and elastin content and internal elastic lamina (IEL) organization. Only adult MUN males developed hypertension (SBP: MUN_{males}=176.6±5.6; $Control_{males}$=136.1±4.9 mmHg). At birth MUN rats were lighter, with smaller aortic cross sectional area (MUN_{males}=1.51±0.08 $x10^5$, $Control_{males}$=2.8±0.04 $x10^5$ μm^2); during lactation MUN males and females exhibited catch-up growth and aortic hypertrophy (MUN_{males}=14.5±0.5 $x10^5$, $Control_{males}$=10.4±0.9 $x10^5$ μm^2), maintained until adulthood. MUN aortas were more compliant until weaning (Beta: MUN_{males}=1.0±0.04; $Control_{males}$=1.3±0.03), containing less collagen with larger IEL fenestrae, returning to normal in adulthood. Purified elastin from young MUN offspring was more compliant in both sexes; only MUN adult females maintained larger elastin compliance (slope: $MUN_{females}$=24.1±1.9; $Control_{females}$=33.3±2.8). Fetal undernutrition induces deficient aortic development followed by hypertrophic remodeling and larger aortic compliance in the perinatal period, with similar alterations in collagen and elastin in both sexes. The observed alterations argue against an initial mechanical cause for sex differences in hypertension development. However, the maintenance of high elastin compliance in adult females might protect them against blood pressure rise.

Abbreviations

CSA. Cross Sectional Area

CVD. Cardiovascular Diseases

DBP. Diastolic Blood Pressure

ECM. Extracellular Matrix

HR. Heart Rate

IUGR. Intrauterine Growth Restriction

IEL. Internal Elastic Lamina

MUN. Maternal Undernutrition

PFA. Paraformaldehyde

SBP. Systolic Blood Pressure

W. Weight

Background

Fetal and perinatal life are critical developmental periods and, if disrupted, may predispose the individual for later development of disease. Epidemiological and experimental studies have shown that suboptimal fetal growth, and subsequent low birth weight, is associated with a higher incidence of cardiovascular risk factors (hypertension, obesity and diabetes) and cardiovascular diseases (CVD) in adult life (Dasinger and Alexander, 2016). Inadequate fetal development, due to maternal malnutrition, placental alterations or exposure to other stress factors during intrauterine life, is frequently accompanied by accelerated postnatal growth, which has been proposed to be a key contributor to the development of CVD (Singhal et al., 2007).

Hypertension is one of the CVD risk factors consistently linked with low birth weight, both in humans and in various experimental animal models (Dasinger and Alexander, 2016). One of the proposed mechanisms to explain the relationship between suboptimal fetal growth and hypertension is a defective vascular development which might alter the mechanical properties of blood vessels (Martyn and Greenwald 1997). In support of this hypothesis is the evidence that low birth weight individuals exhibit a premature stiffening of carotid arteries (Martin et al., 2000), raised blood pressure in early life (Salgado et al., 2009), reduced conduit artery compliance (Martyn et al., 1995), as well as a tendency to remain in the same blood pressure centile during maturation (Voors et al., 1979). The passive mechanical properties of conduit vessels are largely dependent on the extracellular matrix (ECM), in particular on the balance between vascular collagen and elastic fibres and the distribution of tensile forces between them. Collagen and elastic fibres are formed during embryonic development and early postnatal life (Berry et al., 1972; Davis et al., 1995; Wagenseil and Mecham, 2009). Therefore, a defective or unbalanced deposition during these key developmental windows might establish the basis for later development of hypertension. Defective elastogenesis might be particularly important, since after the postnatal developmental period, elastic fibres are not efficiently synthesized, whereas collagen synthesis can be stimulated by several mechanical and humoral stimuli during maturation and ageing (Wagenseil and Mecham, 2009). Furthermore, a deficiency in elastogenesis could also contribute to abnormal wall structure, since elastin guides vascular cellular arrangement during fetal development and its deficit is responsible for abnormal wall formation (Li et al., 1998). In fact, in humans born small, there is evidence of alterations in the structure of the aorta, including reduced lumen size and wall thickening (Skilton et al., 2005).

Fetal programming of hypertension is influenced by sex and it has been shown that females exhibit a certain degree of protection, remaining normotensive or developing milder forms of hypertension (Grigore et al., 2008; Ozaki et al, and Woods et al., 2001). Sex differences in fetal programming of hypertension might be established during fetal development and could be related to the poorer adaptation of the male placenta to an adverse environment (Clifton et al., 2010). Another possibility is the protective effects of female sex hormones on the vasculature (Grigore et al., 2008).

We hypothesize that the sex-dependent development of hypertension in response to fetal undernutrition is related to a lower aortic compliance, due to sex-specific differences in elastogenesis during fetal and perinatal life or in extracellular matrix remodeling during maturation. To test this hypothesis we have used a rat model of fetal nutrient restriction induced by maternal undernutrition during gestation (MUN), in which only male offspring develop hypertension (Rodríguez-Rodríguez et al., 2015 and Rodríguez-Rodríguez et al., 2017). We have established 2 experimental groups (MUN and Control) and compared the following variables in both male and female animals, at 3 age points (birth, weaning period and adult life). The variables analyzed were: 1) blood pressure and heart rate, 2) gross aortic structure and morphology, 3) quasi-static aortic mechanical properties, 4) aortic collagen and elastin content, 5) elastic properties of purified elastin extracted from the aorta and 6) organization of the internal elastic lamina (IEL).

Materials and Methods

Ethical Approval. Experiments were performed on Sprague Dawley rats from the colony maintained in the Animal House at Universidad Autónoma de Madrid (ES-28079-0000097). All experimental procedures conformed to the Guidelines for the Care and Use of Laboratory Animals (NIH publication No. 85-23, revised in 1996) and the Spanish legislation (RD 1201/2005). The experiments were also approved by the Ethics Review Board of Universidad Autónoma de Madrid and by the Comunidad Autónoma de Madrid Review Board for use of Animals for Scientific purposes (RD 53/2013). The experiments were carried out according to the principles and standards for reporting animal experiments in The Journal of Physiology (Grundy, 2015).

Maternal undernutrition (MUN) model. The rats were maintained under controlled conditions (temperature 22°C, relative humidity 40% and 12/12 light/dark photoperiod). The animals were free from any pathogen that might interact with the study outcomes and their welfare was monitored by staff at least once a day.

The model of global nutrient restriction in rats (MUN) was established as previously described (Rodríguez-Rodríguez et al., 2015). The observation of sperm in the vaginal smear in the dams was considered as day 1 of gestation. Thereafter, the dams were allocated either to the Control or MUN experimental groups. During the first 10 days of pregnancy, both Control and MUN rats were fed with the same diet (Euro Rodent breeding Diet 22; 5LF5, Labdiet, Spain) containing 55% carbohydrates, 22% protein, 4.4% fat and 4.1% fiber. From day 11 to the end of gestation MUN rats were provided with 50% of the averaged Control daily intake (previously established as 12g/day). After giving birth, MUN dams were again allowed free access to the diet. The Control rats were given free access to the feed throughout the experimental period. Drinking water was provided *ad libitum* in all cases.

Both MUN and Control dams had litters of 12-15 pups. The pups were sexed and weighed 24 hours after birth and the litters were standardized to 12 individuals, 6 males and 6 females when possible (smaller litters were not used). Experimental procedures were performed on 3 day, 21 day and 6 month old rats. The experiments on 3 day old male rats were carried out in offspring from 3 different MUN dams and 4 Control dams. The experiments on 21 day old and 6 month old rats were carried out in the offspring from 5 different dams. For every variable analyzed, 1-2 males and 1-2 females from each dam were used at every age point studied and the data from the siblings were averaged. The remaining rats from the litter were used for other studies to embody the principles of the 3Rs (replacement, reduction and refinement). All the animals were euthanized by an overdose of anesthesia (see below).

Blood pressure and heart rate. Measurements were made on 21 day and 6 month old rats. The rats were anaesthetized with 37.5mg/kg Ketamine hydrochloride and 0.25 mg/kg Medetomidine hydrochloride i.p. and placed on a heating blanket controlled by a rectal probe. After evaluation of the depth of anesthesia by lack of reflex, the iliac artery was exposed though an incision and a polyethylene P50 catheter, filled with 0.9% saline solution with 1% heparin, was inserted and passed into the distal abdominal aorta. The catheter was connected to a pressure transducer (Statham; Harvard Apparatus) and to a PowerLab data acquisition system/8SP (ADInstruments). The pressure wave was continuously recorded for 45 min and the data were stored for later analysis. In all cases, blood pressure dropped during the first 30 min and thereafter remained stable for the rest of the experimental period. Quantification of heart rate (HR) and diastolic and systolic blood pressure (DBP, SBP) was performed during the last part of the recording period, averaging the data in the pressure wave trace for approximately 1 minute. Thereafter, the rats were killed with excess anesthesia and the thoracic aorta was dissected.

Treatment of the thoracic aorta. The aortic arch was discarded. A ring proximal to the arch was cut, fixed in 4% paraformaldehyde (PFA) and stored for later analysis of aortic structure with confocal microscopy. The adjacent segment, 3-4 mm long, was used to test the mechanical properties of the intact vessel. The remaining thoracic aorta was either fixed with 4% PFA, for the study of IEL organization with confocal microscopy, or treated to remove collagen (see below) to evaluate the mechanical properties of the elastin scaffold. In 3 day old specimens these protocols could not be performed due to insufficient tissue.

In 3 day old rats the mechanical properties of the aorta were assessed with a pressure myograph, this technique being chosen due to the small size of the aorta. The aortas from 21 day and 6 month old animals, as well as the purified elastin scaffolds obtained from them, were too large for pressure ~~by~~ myography and their mechanical properties were evaluated by subjecting rings to isometric tension.

In an additional group of rats the whole thoracic aorta was used to quantify elastin and collagen content.

***Aortic morphology*.** To evaluate gross structure the ring proximal to the aortic arch was used. The ring was mounted on a slide provided with a small well, to avoid compression, containing Citifluor mounting medium (Life Technologies). The rings were visualized with a laser scanning confocal microscope (Leica® TCS SP2) at Ex488 nm/Em500–560 nm, the wavelength at which elastin can be detected by its autofluorescence (Wong and Langille, 1996), thus revealing the limits of the arterial media. Single images were captured with a x20, x10 or x5 air objective

(depending on the size of the artery). Quantification was performed with MetaMorph® image analysis software (Universal Image Corporation). Internal and external perimeters were measured from the images and internal diameters and medial cross sectional medial areas (CSA) were calculated, assuming the sections were circular.

Pressure myography. Aortic segments from 3 day old rats were mounted on a pressure myograph (Danish Myotech P100, J.P. Trading, Denmark), as previously described (Gil-Ortega et al., 2016). Briefly, the arterial segment was secured with nylon sutures between 2 glass cannulae in an organ bath maintained at 37°C, containing zero-calcium physiological salt solution (0Ca-PSS) of the following composition:115 mM NaCl, 4.6 mM KCl, 25 mM $NaHCO_3$, 1.2 mM $KH2PO_4$,1.2 mM $MgSO_4$, 10 mM EGTA, 11 mM glucose and bubbled with a mixture of 95% O_2 and 5% CO_2 to maintain the pH between 7.3 and 7.4. The organ bath was placed on the stage of a Zeiss Axiovert inverted microscope coupled to a CCD camera (Sony XC-73CE, monochrome) attached to the microscope`s third ocular tube. The artery was first allowed to equilibrate for 15 min and thereafter it was exposed to increasing pressures (5, 20, 40, 60, 80, 100, 120 mm Hg). At each pressure, the artery was allowed to stabilize for 3 minutes and an image was taken with a x10 objective. From the images, external diameter was measured with ImageJ software (internal diameters could not be visualized). From each segment a pressure-stretch relationship was calculated. Stretch (λ) was defined as D_x-D_0/D_0, where D_x is the external diameter at each pressure (P) and D_0, the diameter at or near to zero pressure. Individual pressure-stretch data were fitted to an exponential curve ($P=\alpha e^{B\lambda}$), where α is a constant. The B values obtained from the fitted curve were taken as a measure of the functional stiffness. At the end of the experiment the vessel was fixed at 40 mm Hg pressure, the estimated SBP of the rat according to previously obtained data (González et al., 2005) and stored for confocal microscopic analysis of fenestral area in the IEL.

Isometric tension. Mechanical properties of ring specimens were tested using an isometric recording system as previously described (Angus and Wright, 2000). Briefly, the 3 mm long segment was mounted on stiff stainless steel hooks in an organ bath containing 0Ca-PSS at 37°C. One of the hooks was fixed to a methacrylate support leg and the second hook was connected to an isometric force transducer coupled to a recording system PowerLab 8SP (ADInstruments). The arterial segment was allowed to equilibrate for 15 min unstretched on the wire hooks with the spacing between the hooks adjusted so that they were both in contact with the inner wall of the vessel but not generating a measurable force. Thereafter, the separation between the hooks was increased in 200 μm steps with a micrometer and the force generated was recorded after 3 min. This procedure was carried out until tissue failure (21-day

old rats) or at the maximum stretch the system allowed (6 month old rats). From each segment a tension-internal circumference relationship was derived as previously described (Angus and Wright, 2000) from the expression $T_i = ae^{BL}{}_i$, where T_i is the circumferential tension at each stretch level *i*, calculated as $T_i = F_i/2g$, where g is segment length (3 mm) and F_i is the force measured at each stretch level; *a*, is a constant and L_i is the internal circumference at each stretch level, calculated from the individual internal diameters at zero tension (obtained from the ring measurements) and the distance between the hooks. The B values obtained from the exponential fit to the tension length data were taken as a measure of the functional stiffness.
In 6 month old rats, due to the large size of the aorta, the system could not accommodate a stretch level sufficient to cause tissue failure and the tension-internal circumference relationship was fitted to a linear expression. In this case the slope was used as a measure of functional stiffness.

Elastin purification protocols. A hot alkali purification method (adapted from Mecham, 2008) was used. Two protocols were established; one was used for quantitative analysis of elastin and collagen content and the second, to obtain scaffolds of purified elastin for mechanical testing.

Purification method to quantify relative elastin and collagen content. The whole thoracic aorta was dried on a glass slide in an oven, at 65°C, for 30 min and weighed (dry weight). Then, it was immersed in a glass tube containing 500 μl of 0.1N NaOH solution, maintained at 100°C in a water bath while avoiding evaporation. The resulting elastin scaffold was washed twice in distilled water, dried in the oven at 65°C for 30 min and weighed again to obtain the relative elastin weight (elastin weight/aortic dry weight). Preliminary experiments were performed to establish the optimum time of incubation in NaOH. We considered as optimal, the incubation time required to eliminate the cells and collagen from the aorta without visible elastin degradation (maintenance of a fenestrated organization in the lamellae). This was assessed by staining the sample with the nuclear dye DAPI (1:500, 15 min), together with collagen I and collagen III antibodies (Santa Cruz, 1:200, overnight) followed by species-specific secondary antibody staining (Alexa Fluor 647, Molecular Probes, 1:200,60 min). The sample was examined with a laser scanning confocal microscope (Leica® TCS SP2) at Ex 405/Em410–475 nm to visualize cell nuclei, Ex488/Em500–560 nm to visualize elastin autofluorescence and Ex 647/Em665 nm to visualize collagen.

The remaining NaOH solution was used to assess total collagen content using a protocol based on dot blot protein detection on PVDF membranes (BioRad) and Sirius red (Sigma-Aldrich), as previously described (Rodríguez-Rodríguez et al., 2013). From each aorta, the relative elastin

and collagen dry weights were calculated with respect to the aortic dry weight prior to purification.

Purification method to test mechanical properties of the elastin scaffold. In this case, the thoracic aorta segment was exposed to the hot alkali, as described above, without the drying step to minimize manipulation and damage.

NaOH incubation times to purify elastin were identical for female and male aortas.

Fenestral organization in the internal elastic lamina (IEL). The IEL is visible due to the autofluorescent properties of elastin; the IEL is partially folded in relaxed vessels and it is best visualized when fixed under pressure or tension (Briones et al., 2003). In 3-day old rats, the IEL was evaluated in the aorta fixed at 40 mm Hg. In 21 day and 6 month old rats, a group of aortic segments were fixed on the hooks under tension with 4% PFA for 2h. The tension level to achieve a maximal stretch of elastin was calculated from the previously obtained tension-internal circumference data (3.6 mm stretch for 21-day old aorta and at 5.6 mm stretch for 6 month old aorta). The fixed segment was cut open, mounted on a slide with the endothelial side facing up and visualized with the Ex 488/Em500–560 nm emission wavelength. Stacks of serial optical sections (0.5 μm thick) were captured from 3 randomly chosen regions with a x20 oil immersion objective at zoom 8, under identical conditions of laser intensity, brightness and contrast, as previously described (Briones et al., 2003). A maximum intensity projection image was obtained from the stack with Metamorph Image analysis software. These images were segmented at identical threshold levels and binary images obtained to quantify the relative area occupied by the fenestra.

Statistical analysis

Statistical analysis was performed with SPSS (version 22). Sample size was calculated as 10rats per group. This calculation was performed based on blood pressure measurements *in vivo*, which was the parameter which, in our experience, exhibits the highest variability, assuming an alpha type error of 5% and a beta type error of 80%. All the variables analyzed followed a normal distribution (Kolmogorov-Smirnov test). Data are expressed as mean ± SEM and include the mean differences between Control and MUN groups and their confidence intervals (CI, 95%). When 2 or more pups from the same dam were used, the values were averaged and the number of dams was used as “n” value for statistical analysis (Dickinson et al., 2016). Data were analyzed by ANOVA, with maternal nutrition, sex and age as factors.

Results

Body weight. At birth MUN rats were significantly smaller than Controls, both in males and females. MUN pups from both sexes remained significantly lighter at 3 days of age. At the age of 21 days there was no significant difference in body weight between MUN and Control rats, either in males or in females. Again, at the age of 6 months there was no significant difference in body weight between MUN and Control males or females (Figure 1). The interaction between sex and age was statistically significant ($p<0.001$), showing the expected sexual dimorphism in body weight of adult rats from both experimental groups.

Blood pressure and heart rate. At the age of 21 days we found no statistically significant differences in SBP, DBP or HR between MUN and Control rats, either in males or in females. At the age of 6 months MUN males exhibited significantly higher SBP and DBP compared to their age and sex matched Control counterparts. We did not observe statistically significant differences between MUN and Control females. Heart rate was not significantly different between MUN and Control rats, either in males or in females (Figure 2). There was a significant interaction between the 3 factors (sex, age and maternal nutrition) for SBP ($p<0.01$) and DBP ($p<0.05$), but not for HR, which indicates an age-dependent sexual difference in blood pressure in association with maternal nutrition.

Aortic structure. There was no statistical difference between groups in the internal diameter of the aorta at any age studied (Figure 3A). 3-day old MUN males had a significantly smaller medial CSA compared to Controls. At the age of 21 days medial CSA was significantly larger in MUN rats compared to Controls both in males and females. A larger CSA was also found in 6 month old MUN males and females compared to their sex-matched Control counterparts (Figure 3B). A significant interaction between sex and age was observed for both internal diameter ($p<0.001$) and CSA ($p<0.001$), which indicates a sexual dimorphism in the size of the aorta in adult rats from both experimental groups. In addition, a significant interaction between maternal nutrition and age was found for CSA ($p<0.001$); which suggests that maternal undernutrition induces wall hypotrophy during fetal development followed by a hypertrophic response during the catch-up growth period. No differences in the number of elastic lamellae were observed at any age studied (data not shown).

Mechanical tests on the thoracic aorta. In 3 day old MUN male rats the pressure-stretch relationship was shifted to the right and the mean B value, derived from the expression $P=ae^{B\lambda}$, was significantly lower when compared to Controls (Figure 4A).

In 21-day old MUN rats the tension-stretch relationship was shifted to the right and the mean B value (derived from the expression $T_i = ae^{BLi}$) was significantly smaller in MUN rats compared

to Controls, both in males and in females (Figure 4B). No significant interaction was found between maternal nutrition and sex in the B value, indicative of a similar mechanical behavior of young male and female aorta.

In the tension-stretch tests on 6 month old rats it was not possible to reach tissue failure due to the large size of the vessel and limitations of the measurement system. Over the range of stretches investigated there was a linear relationship between tension and stretch. There were no statistically significant differences in the slopes of linear fits to the relationship between MUN and Control rats, either in males or in females (Figure 4C). No significant interaction was found between maternal nutrition and sex in slope values, indicative of a similar mechanical behavior of adult male and female aorta from both experimental groups.

Aortic elastin purification. Experiments were performed to determine the optimum incubation time with hot alkali to obtain elastin scaffolds devoid of cells and collagen. It was observed that after 15 minutes in NaOH the cellular component of the aorta was completely removed, but collagen was still visible in both 21-day old and 6-month old rat aorta. In the aorta from young rats, a 30 min incubation period completely removed collagen and the fenestrae were still visible in the IEL; longer incubation times substantially degraded elastin. In the aorta from adult rats a 45 min period was required to completely eliminate collagen leaving visible fenestra and longer incubation times substantially degraded IEL (Figure 5).

Mechanical tests on purified aortic elastin. In purified elastin scaffolds tension-stretch data exhibited a linear relationship (Figure 6). In 21 day old MUN rats the slope of this relationship had significantly lower values compared to Controls, both in males and in females, showin that the elastin scaffold of MUN rats was more compliant than those of Controls (Figure 6A).

In 6 month old rats there were no statistically significant differences in slope values between MUN and Control males. However, a significantly lower slope value was found in MUN females compared to female Controls (Figure 6B). A significant interaction between sex and age was found for slope values, suggesting that the change with age in the elastin mechanical behavior is influenced by sex.

Collagen and elastin content. At the age of 21 days we did not detect a significant difference in relative elastin content between MUN and Control rats, either in males or in females (Figure 7A). Relative collagen content was significantly smaller in aortas from MUN rats in both males and females (Figure 7B).

At the age of 6 months we did not detect a significant difference between MUN and Control rats in relative elastin or collagen content, either in males or in females (Figure 7).

Fenestral organization in the IEL. In the aorta from 3-day old rats the fenestrae were very small and hardly visible and could not be accurately quantified. In 21 day old aortas the IEL from Control rats appeared denser and more compact compared to the IEL from MUN rats, both in males and females. The area occupied by the fenestrae (relative to that of the entire image) was significantly larger in MUN rats compared to Controls, both in males and in females (Figure 8A).

In 6 month old rats, the fenestrae were larger than in 21 day old rats. No significant differences in the relative fenestral area were observed between groups (MUN and Control), either in males or females. However, a significant interaction between maternal nutrition and sex was found for fenestral area ($p<0.05$), suggesting a different mode of age-related IEL remodeling in MUN males and females.

Discussion

Our main objective was to determine if the sex-dependent development of hypertension induced by nutrient restriction during fetal life could be explained by an early alteration of the mechanical properties of the aorta and to assess the involvement of collagen and elastin alterations. To achieve this objective, we introduced some modifications in the methodology which merit discussion.

Methodological aspects

Collagen and elastin and their interaction are the main determinants of the passive mechanical properties of the large elastic arteries and they are often quantified in vascular research from morphometric analysis of vascular sections stained with specific dyes or antibodies. One of our methodological objectives was to quantify these ECM proteins from the same vascular location with a chemical method, which could be both less time consuming and less subjective than classical histomorphometry. The method is based on the classical method of purification of elastin in hot alkali and the quantification of collagen in the remaining solution. Elastin is the main component of elastic fibres and is highly resistant to high temperature, extreme pH and chemical attack. Several purification methods have been described, including autoclaving, extraction in CnBr or in NaOH at high temperature, each of them with advantages and pitfalls (Mecham, 2008). We chose the hot alkali method for several reasons: 1) the scaffold obtained with this method matches the aminoacid composition of native elastin (Daamen et al., 2001), 2) it allows the assaying of collagen in the resulting solution and 3) it is an easier and less toxic method than CnBr extraction. The main drawback of this approach is the possibility of inducing some fragmentation of elastin. To minimize this problem it has been recommended to avoid prolonged incubation times (Mecham, 2008). Since we were using aorta from rats of different ages we considered it important to establish the optimum incubation time. Our results demonstrate that the cellular component is the first to be eliminated, while collagen requires longer times. We considered the visualization of intact fenestral organization in the IEL as a good means of judging the degree of elastin degradation, based on our previous reports using elastase (Briones et al., 2003) or CnBr purification (Arribas et al., 2008). It is important to note that the purified elastin scaffold obtained for mechanical tests is elastin devoid of the microfibrilar component of the elastic fibre (Daamen et al., 2001) as well as, by definition, alkali soluble elastin, and therefore these specimens might not exhibit the mechanical behavior of the native elastic fibre. Moreover, we cannot be sure that the NaOH digestion has not induced some degree of elastin fragmentation.

The collagen assay in the remaining extract after elastin purification, developed by our group, is based on the detection of the basic residues of the collagen aminoacids with Sirius red on a dot blot assay (Rodríguez-Rodríguez et al., 2013). This method is similar to the Sircol collagen colorimetric assay, previously used to evaluate intact collagen (Dodson et al., 2017). The main advantage of our method is that it enables one to detect all the collagen in the vascular wall, independent of the degree of fragmentation, using gelatin (semi-fragmented collagen) as a standard. Since the method is compatible with the NaOH assay it has the advantage that it allows quantification of total collagen and elastin from the same part of the vessel.

Hemodynamic alterations induced by fetal undernutrition

The present results show that MUN rats from both sexes were normotensive at weaning and only adult MUN males developed hypertension. These data confirm the sexual differences in blood pressure development in rats exposed to global nutrient restriction during fetal life, as has been previously described by others and by us (Dasinger and Alexander, 2016; Rodriguez-Rodriguez et al., 2017). We analyzed blood pressure under medetomidine/ketamine anesthesia, which needs to be taken into consideration since both drugs exert cardiovascular effects. In small animals ketamine has been shown to induce a short term increase in blood pressure (Dobromylskyj, 1996), an effect related to increased sympathetic nervous system outflow. Consequently, ketamine produces cardiovascular effects that resemble sympathetic nervous system stimulation. On the other hand, medetomidine has alpha 2-adrenergic agonist effects reducing noradrenaline outflow within the central nervous system, which results in dampening of the central sympathetic tone and bradycardia (Sinclair, 2003). In fact, we have evidence of a lower HR in MUN and Control rats under medetomidine/ketamine anesthesia compared to diacepam/ketamine (Rodriguez-Rodriguez et al., 2017). Under our experimental conditions, using a mixture of both anesthetics, we observed an initial pressure drop that stabilized after 30 minutes. This effect was observed in all animals, irrespective of their dietary group. Since alterations in the sympathetic nervous system have been described in animal models of fetal programming (Alexander et al., 2015), we cannot disregard the possibilitythat the anesthetics used might exert different cardiovascular effects in MUN and Control rats. Furthermore, we cannot exclude the possibility of a different effect of the anesthesia on males and females which might have masked a mild form of hypertension in MUN females, as previously described (Dassinger and Alexander, 2016). It also needs to be pointed out that we did not evaluate the stage of estrus cycle of the rat when the blood pressure measurements were performed. This might influence hemodynamic variables, since estrogens are known to induce vasorelaxation, through a positive modulation of nitric oxide production (Chakrabarti et al., 2013).

Structural and mechanical alterations induced by fetal undernutrition

Our main objective was to evaluate the hypothesis that sex-dependent programming of hypertension induced by fetal nutrient restriction is related to deficient elastogenesis and subsequent perinatal alteration of aortic mechanical properties.

Fetal undernutrition induced a poor vascular development, as demonstrated by the smaller aorta in newborn MUN male rats. This initial effect was followed by a hypertrophic response observed at weaning, likely related to accelerated growth during the lactation period. This is a compensatory response to nutrient deficiency *in utero* which we have previously observed in other organs, such as adipose tissue (Muñoz-Valverde et al., 2015) and the heart (Rodríguez-Rodríguez et al., 2017). Vascular remodeling in the aorta was not accompanied by increased vessel stiffness in early life. In fact, the aorta from MUN rats was less stiff at birth, as shown by the rightward shift of the stretch-pressure relationships and the lower B values. Moreover, the reduced stiffness was maintained at the age of 21 days. Our data differ from those recently reported in a rat model of IUGR induced by bilateral uterine artery ligation, which show an increased stiffness of the aorta at weaning (Dodson et al., 2017). Another difference between both studies is the alteration in elastin. In the rat model of placental insufficiency Dodson and co-workers reported a reduction in the number of elastic lamella, while we did not detect alterations in elastin content or in the number of lamella. We suggest that differences in haemodynamic environment might account for the observed disparity between the two models of IUGR, since elastogenesis is highly influenced by local hemodynamic conditions. The key role of placental flow on elastin deposition is shown in necropsies from children born with a single umbilical artery in which the entire placental blood flow passes through the common iliac artery on one side only. This vessel exhibited a lamellar structure richer in elastin compared to the contralateral artery which had not been included in the placental circulation (Meyer and Lind, 1974). In a study on adolescents born with a single umbilical artery, a large difference was found in the compliance of the two iliac arteries, assessed by measurements of pulse wave velocity, thus demonstrating that the effect of abnormal blood flow during uterine life has long lasting effects on arterial structure and function (Berry et al., 1976).

Despite the fact that we did not observe modifications in elastin content or number of lamella, a less compact organization of the IEL with larger fenestral area was found in MUN rats. We cannot discard the possibility that this alteration reflects a reduced elastin deposition, not detectable by relative elastin weight measurements. Alterations in elastin distribution in lamella, showing a reduction in inter-lamella connections, have been previously found in blood vessels from young rats exposed to protein restriction in fetal life (Khorram et al., 2007). In

SHR and WKY rats we have previously reported a positive association between fenestral size and vascular compliance of purified elastin frameworks from aorta (Arribas et al., 2008). Therefore, we suggest that the observed alterations in the IEL organization might contribute to the reduced stiffness of the purified elastin scaffolds in 21-day old MUN rats, evidenced by the lower slope values of the stretch-tension relationship.

Collagen is, together with elastin, another key ECM determinant for the passive vascular mechanical properties. Therefore, the lower collagen content of the aorta from young MUN rats could contribute to the observed reduction in stiffness. Taking together our current data and previous reports in other rat models of IUGR, we note an important difference in the deposition of ECM, particularly elastin and collagen, between models of placental insufficiency and those of nutritional deficiency. These might account for the observed disparity in the vascular mechanical properties of young animals in each of these experimental models. The observed structural and mechanical alterations induced by nutrient deficit were similar in 21-day old male and female offspring. Therefore, our results argue against an early mechanical defect induced by altered elastogenesis as primary cause of sex-dependent hypertension in this rat model of IUGR.

The initially reduced stiffness of the aorta from MUN rats was lost by the time they reached adulthood. Due to methodological constraints, we were unable to evaluate the mechanical properties of the aorta over the full range of stretch. The stretch-tension relationship in 6-month old aortas was approximately linear, which suggests that we reached only a limited degree of elastin deformation and thus it is likely that we did not reach a significant level of collagen recruitment (Dobrin, 1978). Therefore, we cannot provide information on the contribution of collagen to the mechanical properties of the aorta from adult rats or possible differences between MUN and Control animals. Although we did not detect alterations in total collagen content, we cannot rule out a modification in the organization of collagen fibres. In this regard changes in the angular distribution of adventitial collagen have been previously described in a sheep model of IUGR (Dodson et al., 2014). This is a limitation in this study, which deserves further analysis with appropriate methodology.

The relative elastin content in the adult aorta was maintained at a similar level to that in 21-day old rats, (around 40% of dry weight), similar values to those previously reported in rats (Greenwald and Berry, 1978) and mice (Davis et al., 1995). These data confirm that elastin is not actively synthesized after weaning and it is mainly remodeled, as shown by the observed enlargement of the IEL fenestrae from the age of 21 days to adulthood. This has been previously reported in rabbit conduit (Wong and Langille, 1996) and in rat resistance arteries (González et al., 2005). Elastin content was similar in males and females, but a sex difference

was observed in the remodeling of the IEL; i.e. the increased fenestral size with maturation was greater in the female aorta. This was accompanied by a larger compliance of elastin, demonstrated by the lower slope values of elastin scaffolds in female aorta, particularly in MUN rats. In adults, it was also found that the larger compliance of the elastin scaffolds observed at a young age was maintained in MUN females but not in MUN males. Fenestral enlargement is induced by metalloproteases (MMPs), particularly MMP-2 (Jackson et al., 2002), which are regulated by sex steroids (Vassilev et al., 2005). Therefore, it is possible that elastin remodeling in MUN rats is influenced by sex hormones. In fact, sex steroids have been proposed to play a role in the different responses of males and females to fetal stress. Testosterone has been shown to be implicated in fetal programming of hypertension, while estrogens provide protection to females exposed to several fetal insults (Ojeda et al., 2007a; Ojeda et al., 2007b). The differences in the mechanical properties of elastin between male and female MUN rats, observed in adult life, but not in the perinatal period (before sexual maturation), also support this assumption. Therefore, it is possible that estrogens contribute to the protection of females against fetal programming of hypertension through a more effective mechanical adaptation during adult life.

References

ALEXANDER, B., DASINGER, J., INTAPAD, S., 2015. Fetal programming and cardiovascular pathology. *Comprehensive Physiology*; **5**(2), pp. 997-1025.

ANGUS, J.A. and WRIGHT, C.E., 2000. Techniques to study the pharmacodynamics of isolated large and small blood vessels. *Journal of pharmacological and toxicological methods,* **44**(2), pp. 395-407.

ARRIBAS, S.M., BRIONES, A.M., BELLINGHAM, C., GONZALEZ, M.C., SALAICES, M., LIU, K., WANG, Y. and HINEK, A., 2008. Heightened aberrant deposition of hard-wearing elastin in conduit arteries of prehypertensive SHR is associated with increased stiffness and inward remodeling. *American journal of physiology.Heart and circulatory physiology,* **295**(6), pp. H2299-307.

BERRY, C., LOOKER, T. and GERMAIN, J., 1972. Nucleic acid and scleroprotein content of the developing human aorta. *The Journal of pathology,* **108**(4), pp. 265-274.

BERRY, C.L., GOSLING, R.G., LAOGUN, A.A. and BRYAN, E., 1976. Anomalous iliac compliance in children with a single umbilical artery. *British heart journal,* **38**(5), pp. 510-515.

BRIONES, A.M., GONZÁLEZ, J.M., SOMOZA, B., GIRALDO, J., DALY, C.J., VILA, E., CARMEN GONZÁLEZ, M., MCGRATH, J.C. and ARRIBAS, S.M., 2003. Role of elastin in spontaneously hypertensive rat small mesenteric artery remodelling. *The Journal of physiology,* **552**(1), pp. 185-195.

CHAKRABARTI, S., MORTON, J.S., DAVIDGE, S.T., 2014. Mechanisms of estrogen effects on the endothelium: an overview. *Canadian Journal of Cardiology,***30**(7), pp.705-12.

CLIFTON, V., 2010. Sex and the human placenta: mediating differential strategies of fetal growth and survival. *Placenta,* **31**, pp. S33-S39.

DAAMEN, W., HAFMANS, T., VEERKAMP, J. and VAN KUPPEVELT, T., 2001. Comparison of five procedures for the purification of insoluble elastin. *Biomaterials,* **22**(14), pp. 1997-2005.

DASINGER, J.H. and ALEXANDER, B.T., 2016. Gender differences in developmental programming of cardiovascular diseases. *Clinical science (London, England : 1979),* **130**(5), pp. 337-348.

DAVIS, E.C., 1995. Elastic lamina growth in the developing mouse aorta. *The journal of histochemistry and cytochemistry: official journal of the Histochemistry Society,* **43**(11), pp. 1115-1123.

DICKINSON, H., MOSS, T.J., GATFORD, K.L., MORITZ, K.M., AKISON, L., FULLSTON, T., HRYCIW, D.H., MALONEY, C.A., MORRIS, M.J., WOOLDRIDGE, A.L., SCHJENKEN, J.E., ROBERTSON, S.A., WADDELL, B.J., MARK, P.J., WYRWOLL, C.S., ELLERY, S.J., THORNBURG, K.L., MUHLHAUSLER, B.S., MORRISON, J.L., 2016. A review of fundamental principles for animal models of DOHaD research: an Australian perspective. *J Dev Orig Health Dis* **7**, pp. 449-472.

DOBRIN, P.B., 1978. Mechanical properties of arterises. *Physiological Reviews,* **58**(2), pp. 397-460.

DODSON, R.B., MILLER, T.A., POWERS, K., YANG, Y., YU, B., ALBERTINE, K.H. and ZINKHAN, E.K., 2017. Intrauterine growth restriction influences vascular remodeling and stiffening in the weanling rat more than sex or diet. *American journal of physiology.Heart and circulatory physiology,* **312**(2), pp. H250-H264.

DODSON, R.B., ROZANCE, P.J., PETRASH, C.C., HUNTER, K.S. and FERGUSON, V.L., 2014. Thoracic and abdominal aortas stiffen through unique extracellular matrix changes in intrauterine growth restricted fetal sheep. *American journal of physiology.Heart and circulatory physiology,* **306**(3), pp. H429-37.

DOBROMYLSKYJ, P., 1996. Cardiovascular changes associated with anaesthesia induced by medetomidine combined with ketamine in cats. *Journal of Small Animal Practice* **37**(4), pp. 169-172.

GIL-ORTEGA, M., MARTÍN-RAMOS, M., ARRIBAS, S.M., GONZÁLEZ, M.C., ARÁNGUEZ, I., RUIZ-GAYO, M., SOMOZA, B. and FERNÁNDEZ-ALFONSO, M.S, 2016. Arterial stiffness is associated with adipokine dysregulation in non-hypertensive obese mice. *Vascular Pharmacology,* **77***,* pp. 38-47.

GONZÁLEZ, J.M., BRIONES, A.M., STARCHER, B., CONDE, M., SOMOZA, B., DALY, C., VILA, E., MCGRATH, I., GONZÁLEZ, M.C. and ARRIBAS, S.M., 2005. Influence of elastin on rat small artery mechanical properties. *Experimental physiology,* **90**(4), pp. 463-468.

GREENWALD, S. and BERRY, C., 1978. Static mechanical properties and chemical composition of the aorta of spontaneously hypertensive rats: a comparison with the effects of induced hypertension. *Cardiovascular research,* **12**(6), pp. 364-372.

GRIGORE, D., OJEDA, N.B. and ALEXANDER, B.T., 2008. Sex differences in the fetal programming of hypertension. *Gender medicine,* **5**, pp. S121-S132.

GRUNDY, D., 2015 Principles and standards for reporting animal experiments in The journal of Physiology and Experimental Physiology. *The Journal of Physiology***593**(12), pp.2547-2549.

JACKSON, Z.S., GOTLIEB, A.I. and LANGILLE, B.L., 2002. Wall tissue remodeling regulates longitudinal tension in arteries. *Circulation research,* **90**(8), pp. 918-925.

KHORRAM, O., MOMENI, M., DESAI, M. and ROSS, M.G., 2007. Nutrient restriction in utero induces remodeling of the vascular extracellular matrix in rat offspring. *Reproductive sciences (Thousand Oaks, Calif.),* **14**(1), pp. 73-80.

LI, D.Y., BROOKE, B., DAVIS, E.C. and MECHAM, R.P., 1998. Elastin is an essential determinant of arterial morphogenesis. *Nature,* **393**(6682), pp. 276.

MARTIN, H., HU, J., GENNSER, G. and NORMAN, M., 2000. Impaired endothelial function and increased carotid stiffness in 9-year-old children with low birthweight. *Circulation,* **102**(22), pp. 2739-2744.

MARTYN, C. and GREENWALD, S., 1997. Impaired synthesis of elastin in walls of aorta and large conduit arteries during early development as an initiating event in pathogenesis of systemic hypertension. *The Lancet,* **350**(9082), pp. 953-955.

MARTYN, C.N., BARKER, D.J., JESPERSEN, S., GREENWALD, S., OSMOND, C. and BERRY, C., 1995. Growth in utero, adult blood pressure, and arterial compliance. *British heart journal,* **73**(2), pp. 116-121.

MECHAM, R.P., 2008. Methods in elastic tissue biology: elastin isolation and purification. *Methods,* **45**(1), pp. 32-41.

MEYER, W.W. and LIND, J., 1974. Iliac arteries in children with a single umbilical artery. Structure, calcifications, and early atherosclerotic lesions. *Archives of Disease in Childhood,* **49**(9), pp. 671-679.

MUNOZ-VALVERDE, D., RODRÍGUEZ-RODRÍGUEZ, P., GUTIERREZ-ARZAPALO, P., LOPEZ DE PABLO, A.L., GONZÁLEZ, M.C., LOPEZ-GIMENEZ, R., SOMOZA, B. and ARRIBAS, S., 2015. Effect of fetal undernutrition and postnatal overfeeding on rat adipose tissue and organ growth at early stages of postnatal development. *Physiological Research,* **64**(4), pp. 547.

OJEDA, N.B., GRIGORE, D., ROBERTSON, E.B. and ALEXANDER, B.T., 2007a. Estrogen protects against increased blood pressure in postpubertal female growth restricted offspring. *Hypertension,* **50**(4), pp. 679-685.

OJEDA, N.B., GRIGORE, D., YANES, L.L., ILIESCU, R., ROBERTSON, E.B., ZHANG, H. and ALEXANDER, B.T., 2007b. Testosterone contributes to marked elevations in mean arterial pressure in adult male intrauterine growth restricted offspring. *American journal of physiology.Regulatory, integrative and comparative physiology,* **292**(2), pp. R758-63.

OZAKI, T., NISHINA, H., HANSON, M. and POSTON, L., 2001. Dietary restriction in pregnant rats causes gender-related hypertension and vascular dysfunction in offspring. *The Journal of physiology,* **530**(1), pp. 141-152.

RODRÍGUEZ-RODRÍGUEZ, P., ARRIBAS, S.M., LÓPEZ DE PABLO, A.L., GONZÁLEZ, M.C., ABDERRAHIM, F. and CONDEZO-HOYOS, L., 2013. A simple dot-blot–Sirius red-based assay for collagen quantification. *Analytical and bioanalytical chemistry,* **405**(21), pp. 6863-6871.

RODRÍGUEZ-RODRÍGUEZ, P., LÓPEZ DE PABLO, A.L., GARCÍA-PRIETO, C.F., SOMOZA, B., QUINTANA-VILLAMANDOS, B., DE DIEGO, JOSÉ J GÓMEZ, GUTIERREZ-ARZAPALO, P.Y., RAMIRO-CORTIJO, D., GONZÁLEZ, M.C. and ARRIBAS, S.M., 2017. Long term effects of fetal undernutrition on rat heart. Role of hypertension and oxidative stress. *PloS one,* **12**(2), pp. e0171544.

RODRÍGUEZ-RODRÍGUEZ, P., LÓPEZ DE PABLO, A.L., CONDEZO-HOYOS, L., MARTÍN-CABREJAS, M.A., AGUILERA, Y., RUIZ-HURTADO, G., GUTIERREZ-ARZAPALO, P.Y., RAMIRO-CORTIJO, D., FERNÁNDEZ-ALFONSO, M.S. and DEL CARMEN GONZÁLEZ, M., 2015. Fetal undernutrition is associated with perinatal sex-dependent alterations in oxidative status. *The Journal of nutritional biochemistry,* **26**(12), pp. 1650-1659.

SALGADO, C.M., JARDIM, PAULO CÉSAR BRANDÃO VEIGA, TELES, F.B.G. and NUNES, M.C., 2009. Low birth weight as a marker of changes in ambulatory blood pressure monitoring. *Arquivos Brasileiros de Cardiologia,* **92**(2), pp. 113-121.

SINCLAIR, M.D., 2003. A review of thephysiological effects of alpha2-agonists related to theclinical use of medetomidine in small animal practice. *Canadian Veterinary Journal,* **44**(11), pp. 885-897.

SINGHAL, A., COLE, T.J., FEWTRELL, M., KENNEDY, K., STEPHENSON, T., ELIAS-JONES, A. and LUCAS, A., 2007. Promotion of faster weight gain in infants born small for gestational age: is there an adverse effect on later blood pressure? *Circulation,* **115**(2), pp. 213-220.

SKILTON, M.R., EVANS, N., GRIFFITHS, K.A., HARMER, J.A. and CELERMAJER, D.S., 2005. Aortic wall thickness in newborns with intrauterine growth restriction. *The Lancet,* **365**(9469), pp. 1484-1486.

VASSILEV, V., PRETTO, C.M., CORNET, P.B., DELVAUX, D., EECKHOUT, Y., COURTOY, P.J., MARBAIX, E. and HENRIET, P., 2005. Response of matrix metalloproteinases and tissue inhibitors of metalloproteinases messenger ribonucleic acids to ovarian steroids in human endometrial explants mimics their gene-and phase-specific differential control in vivo. *The Journal of Clinical Endocrinology & Metabolism,* **90**(10), pp. 5848-5857.

VOORS, A.W., WEBBER, L.S. and BERENSON, G.S., 1979. Time course studies of blood pressure in children-the Bogalusa Heart Study. *American Journal of Epidemiology,* **109**(3), pp. 320-334.

WAGENSEIL, J.E. and MECHAM, R.P., 2009. Vascular extracellular matrix and arterial mechanics. *Physiological Reviews,* **89**(3), pp. 957-989.

WONG, L.C. and LANGILLE, B.L., 1996. Developmental remodeling of the internal elastic lamina of rabbit arteries: effect of blood flow. *Circulation research,* **78**(5), pp. 799-805.

WOODS, L.L., INGELFINGER, J.R. and RASCH, R., 2005. Modest maternal protein restriction fails to program adult hypertension in female rats. *American journal of physiology.Regulatory, integrative and comparative physiology,* **289**(4), pp. R1131-6.

Additional information

Funding sources. Ministerio de Economía y Competitividad-Spain (Grant number FEM2015-63631-R).

There are no competing interests.

Author contributions

Perla Y Gutiérrez-Arzapalo: Vascular structure, isometric tension and elastin quantification experiments, data processing, interpretation and graphs.

Pilar Rodríguez-Rodríguez: Maintenance of the experimental animals, organization of the time points of study, dissections, pressure myography experiments.

David Ramiro-Cortijo: Confocal microscopy experiments and morphometric analysis.

Ángel L López de Pablo: Design of experimental protocols, blood pressure measurements, manuscript writing.

Mª Rosario López-Giménez: Design of data base, statistics and data interpretation.

Luis Condezo-Hoyos: Development of collagen quantification method, experiments of collagen quantification and interpretation of data.

Stephen E Greenwald: interpretation of data on vascular mechanical properties and manuscript writing.

Mª Carmen González: Design of experimental protocols, blood pressure data processing, interpretation and graphs.

Silvia M Arribas: Funding, design of experimental work and manuscript writing.

All authorslisted here qualify for authorship, agree to be accountable for their part of the work and have approved the final version of the manuscript.

Figure legends

Figure 1. Body weight in male and female rats aged 24 h, 3 days, 21 days and 6 months. MUN, maternal undernutrition. In parentheses is shown the number of dams (from each dam 2 pups of each sex were averaged, with the exception of 24h data which includes all pups from each dam). Bar graphs represent the mean and error bars are SEM. Mean differences between Control and MUN groups are shown below each graph together with confidence intervals (*$p<0.05$ when compared to sex and age-matched Control rats).

Figure 2. Systolic and diastolic blood pressure (SBP, DBP) and heart rate (HR) measured in anesthetized male and female rats aged 21 days and 6 months. MUN, maternal undernutrition. In parentheses is shown the number of dams (from each dam 2 pups of each sex were averaged). Bar graphs represent the mean and error bars are SEM. Mean differences between Control and MUN groups are shown below each graph together with confidence intervals (*$p<0.05$ when compared to sex and age matched Control rats).

Figure 3. Thoracic aorta structure. (A) Internal diameter and (B) Media Cross Sectional Area (CSA) from thoracic aorta rings without tension. MUN, maternal undernutrition. In parentheses is shown the number of dams (from each dam 2 pups of each sex were averaged). Bar graphs represent the mean and error bars are SEM. Mean differences between Control and MUN groups are shown below each graph together with confidence intervals (*$p<0.05$ when compared to sex and age matched Control rats).

Figure 4. Mechanical properties of rat aortic segments. (A) Average stretch-pressure relationship in 3-day old rats. (B) Average stretch-tension relationship in 21-day old rats. (C) Average stretch-tension relationship in 6-month old rats. Inset shows the average B values or slope (derived for the exponential fit) from each experimental group. MUN, maternal undernutrition. In parentheses is shown the number of dams (from each dam 2 pups of each sex were averaged). Bar graphs represent the mean and error bars are SEM. Mean differences between Control and MUN groups are shown below each graph together with confidence intervals (*$p<0.05$ when compared to sex and age matched Control rats).

Figure 5. Effect of different incubation times with NaOH on aortic collagen and elastin degradation. Representative images of adventitial collagen and internal elastic lamina from a 21 day old Control rat aorta incubated with 0.1 N NaOH at 0, 15, 30 or 45 minutes. Images were obtained with a laser scanning confocal microscope at Ex488 nm/Em500–560 nm to visualize elastin and Ex 647/Em 665 to visualize collagen, using a x20 objective with zoom 4. Scale bar 25 μm.

Figure 6. Mechanical tests on purified aortic elastin. (A) Average stretch-tension relationship in 21-day old rat aorta. (B) Average stretch-tension relationship in 6-month old rat aorta. Inset shows the average slope values. MUN, maternal undernutrition. In parentheses is shown the number of dams (2 pups from each dam were used). Bar graphs represent the mean and error bars are SEM. Mean differences between Control and MUN groups are shown below each graph together with confidence intervals (*$p<0.05$ when compared to sex and age matched Control rats).

Figure 7. Relative aortic scleroprotein content. (A) Elastin and (B) Collagen. MUN, maternal undernutrition. W, weight. In parentheses is shown the number of dams (from each dam 1-2 pups of each sex were averaged). Bar graphs represent the mean and error bars are SEM. Mean differences between Control and MUN groups are shown below each graph together with confidence intervals (*$p<0.05$ when compared to sex and age matched Control rats).

Figure 8. Internal elastic lamina organization in rat aorta. Relative area of fenestrae and representative confocal images of the internal elastic lamina of 21-day old (A) and 6-month old animals (B). MUN, maternal undernutrition. Images were obtained with a x20 objective, zoom 8 (Scale bar, 100 μm). The relative area of fenestra (area of fenestra relative to the entire image) was measured from binary images. In parentheses is shown the number of dams (from each dam 1-2 pups of each sex were averaged). Bar graphs represent the mean and error bars are SEM. Mean differences between Control and MUN groups are shown below each graph together with confidence intervals (*$p<0.05$ when compared to sex-matched Control rats).

Figure 1

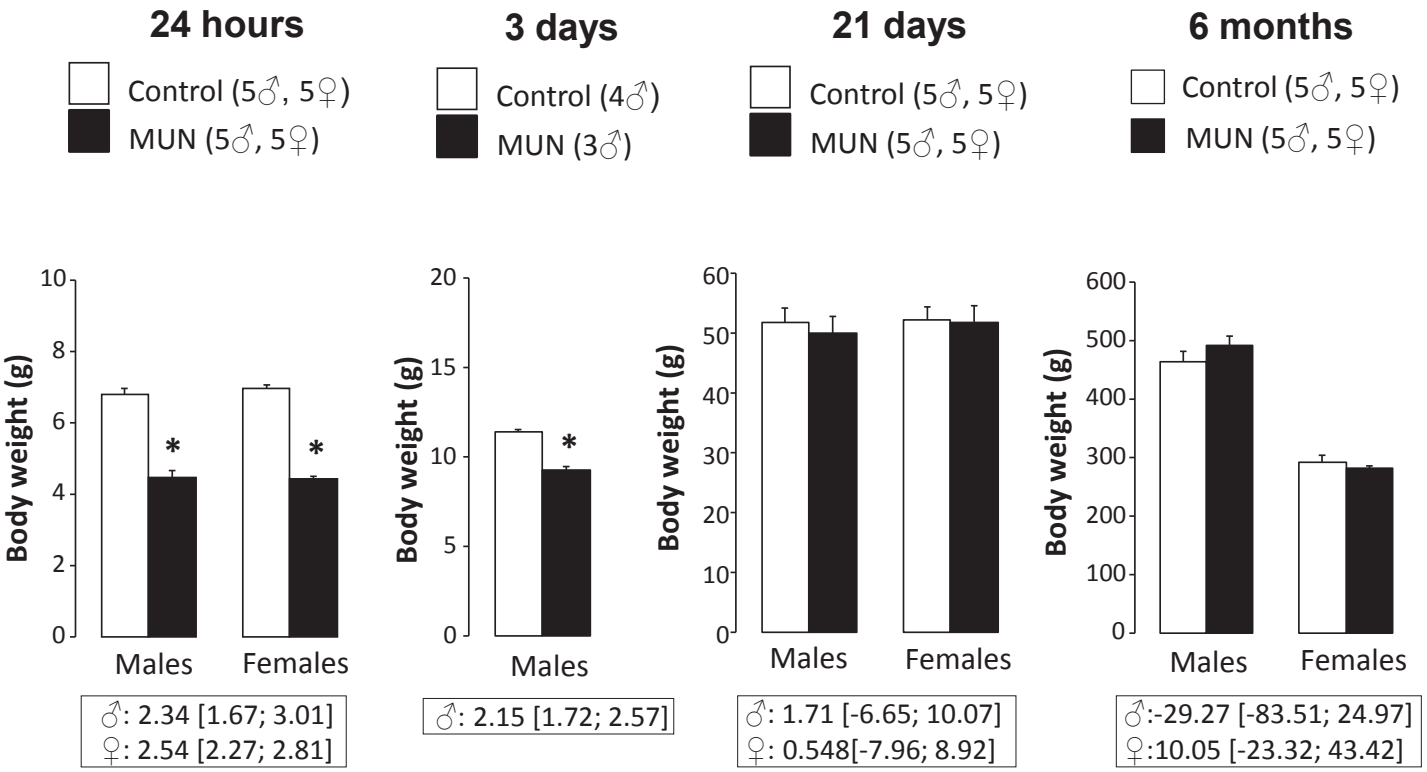
24 hours
Control (5♂, 5♀)
MUN (5♂, 5♀)
Body weight (g)
10
8
6
4
2
0
*
*
Males
Females
♂: 2.34 [1.67; 3.01]
♀: 2.54 [2.27; 2.81]
3 days
Control (4♂)
MUN (3♂)
Body weight (g)
20
15
10
5
0
*
Males
♂: 2.15 [1.72; 2.57]
21 days
Control (5♂, 5♀)
MUN (5♂, 5♀)
Body weight (g)
60
50
40
30
20
10
0
Males
Females
♂: 1.71 [-6.65; 10.07]
♀: 0.548[-7.96; 8.92]
6 months
Control (5♂, 5♀)
MUN (5♂, 5♀)
Body weight (g)
600
500
400
300
200
100
0
Males
Females
♂:-29.27 [-83.51; 24.97]
♀:10.05 [-23.32; 43.42]

Figure 2

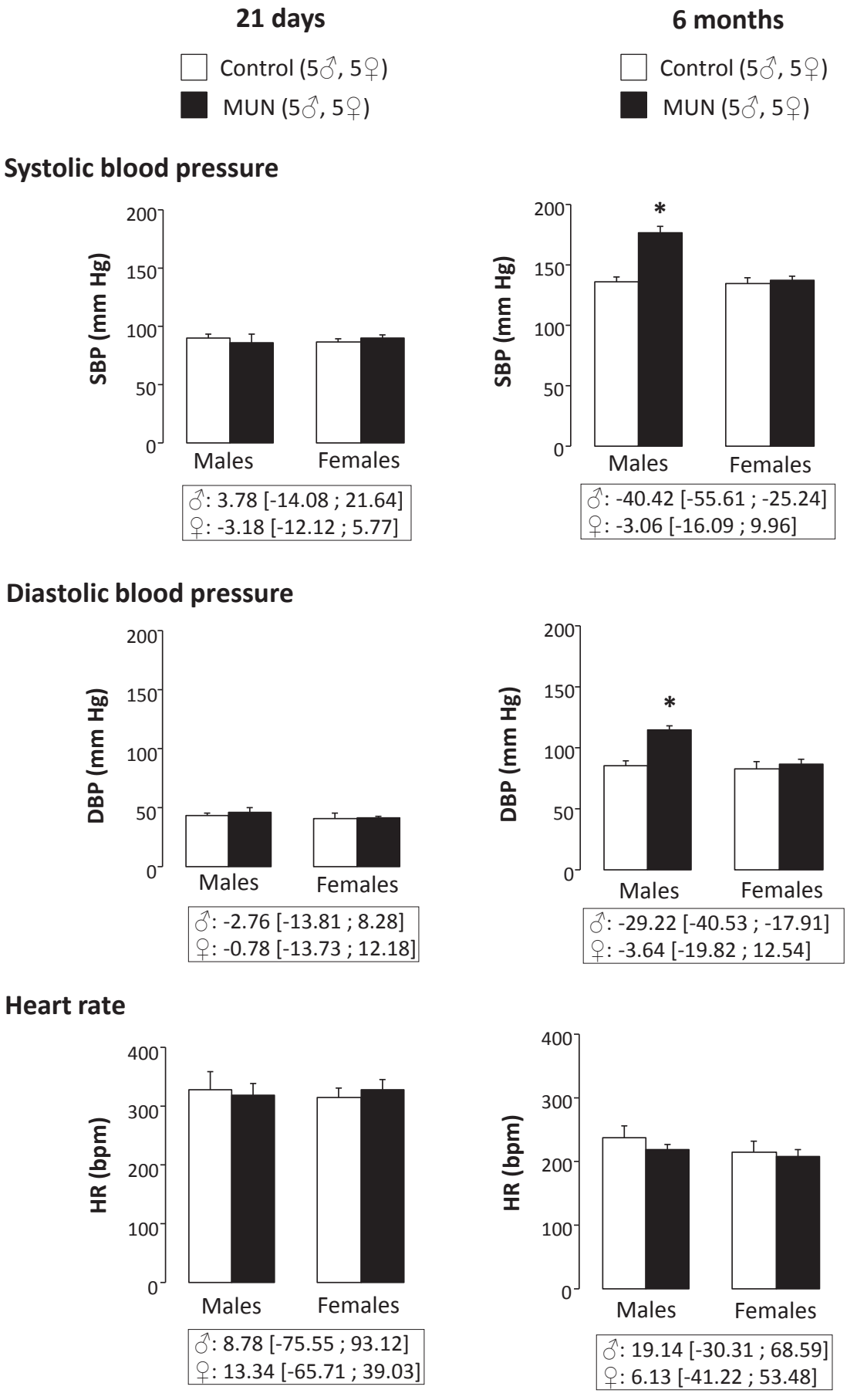
21 days
6 months
Control (5♂, 5♀)
MUN (5♂, 5♀)
Control (5♂, 5♀)
MUN (5♂, 5♀)
Systolic blood pressure
SBP (mm Hg)
200
150
100
50
0
Males
Females
♂: 3.78 [-14.08 ; 21.64]
♀: -3.18 [-12.12 ; 5.77]
*
SBP (mm Hg)
Males
Females
♂: -40.42 [-55.61 ; -25.24]
♀: -3.06 [-16.09 ; 9.96]
Diastolic blood pressure
DBP (mm Hg)
Males
Females
♂: -2.76 [-13.81 ; 8.28]
♀: -0.78 [-13.73 ; 12.18]
*
DBP (mm Hg)
Males
Females
♂: -29.22 [-40.53 ; -17.91]
♀: -3.64 [-19.82 ; 12.54]
Heart rate
HR (bpm)
400
300
200
100
0
Males
Females
♂: 8.78 [-75.55 ; 93.12]
♀: 13.34 [-65.71 ; 39.03]
HR (bpm)
Males
Females
♂: 19.14 [-30.31 ; 68.59]
♀: 6.13 [-41.22 ; 53.48]

Figure 3

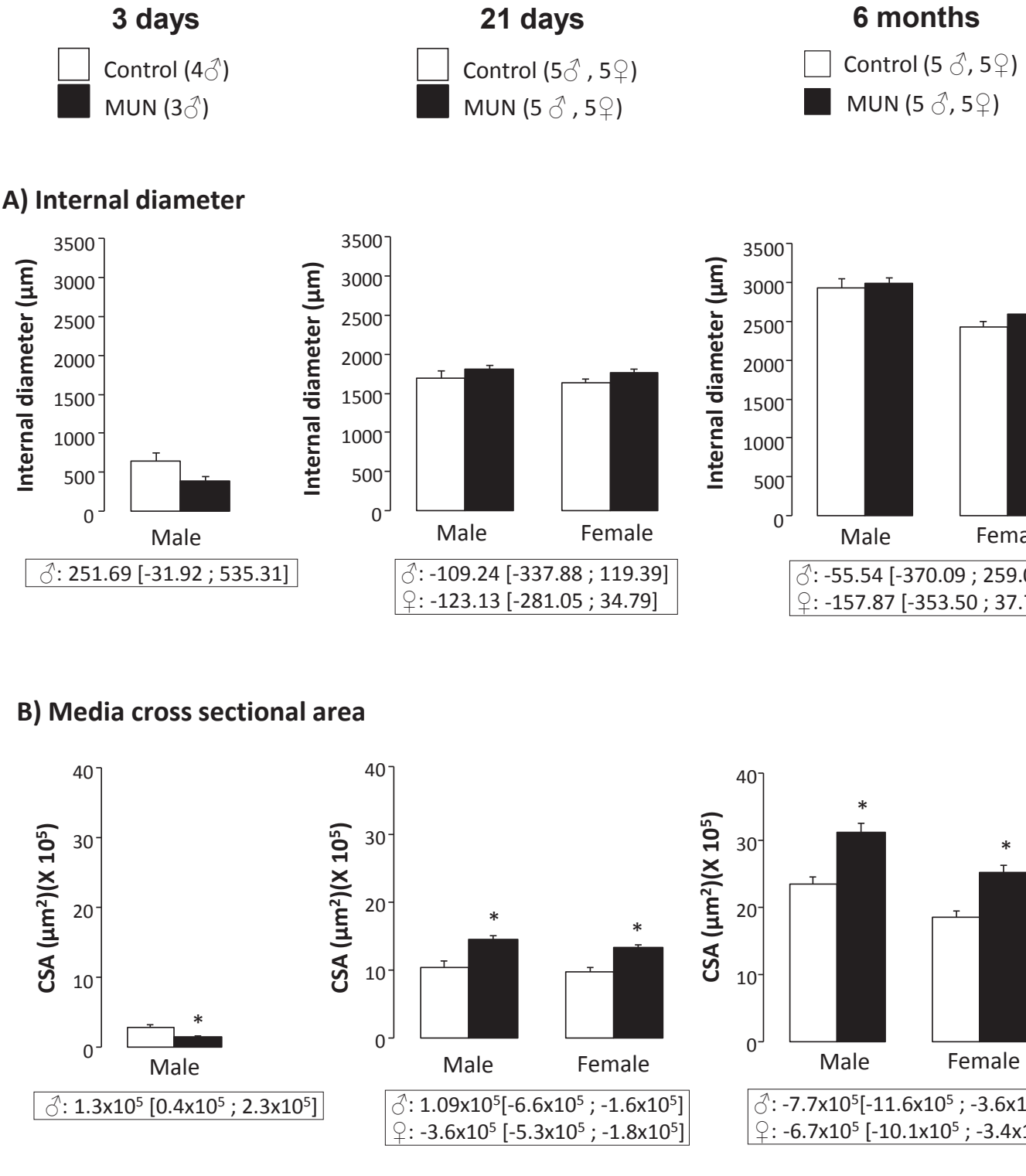
3 days
Control (4♂)
MUN (3♂)
21 days
Control (5♂ , 5♀)
MUN (5 ♂ , 5♀)
6 months
Control (5 ♂, 5♀)
MUN (5 ♂, 5♀)
A) Internal diameter
Internal diameter (µm)
3500
3000
2500
2000
1500
1000
500
0
Male
♂: 251.69 [-31.92 ; 535.31]
Female
♂: -109.24 [-337.88 ; 119.39]
♀: -123.13 [-281.05 ; 34.79]
♂: -55.54 [-370.09 ; 259.01]
♀: -157.87 [-353.50 ; 37.76]
B) Media cross sectional area
CSA (µm²)(X 10⁵)
40
30
20
10
0
*
♂: 1.3x10⁵ [0.4x10⁵ ; 2.3x10⁵]
♂: 1.09x10⁵[-6.6x10⁵ ; -1.6x10⁵]
♀: -3.6x10⁵ [-5.3x10⁵ ; -1.8x10⁵]
♂: -7.7x10⁵[-11.6x10⁵ ; -3.6x10⁵]
♀: -6.7x10⁵ [-10.1x10⁵ ; -3.4x10⁵]

Figure 4

A) Stretch-pressure 3 days aorta

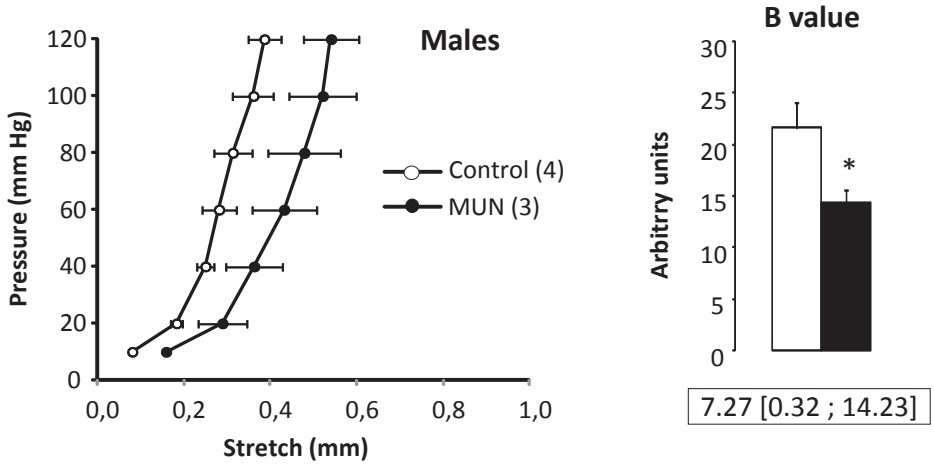

B) Stretch-tension 21 days aorta

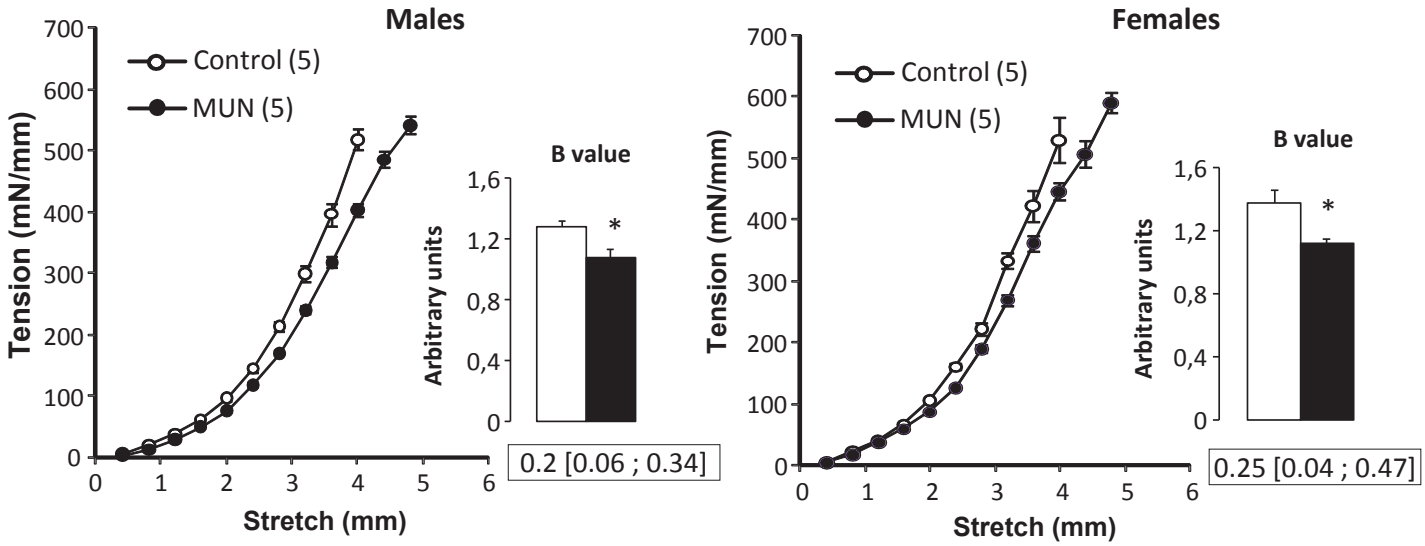

C) Stretch-tension 6 months aorta

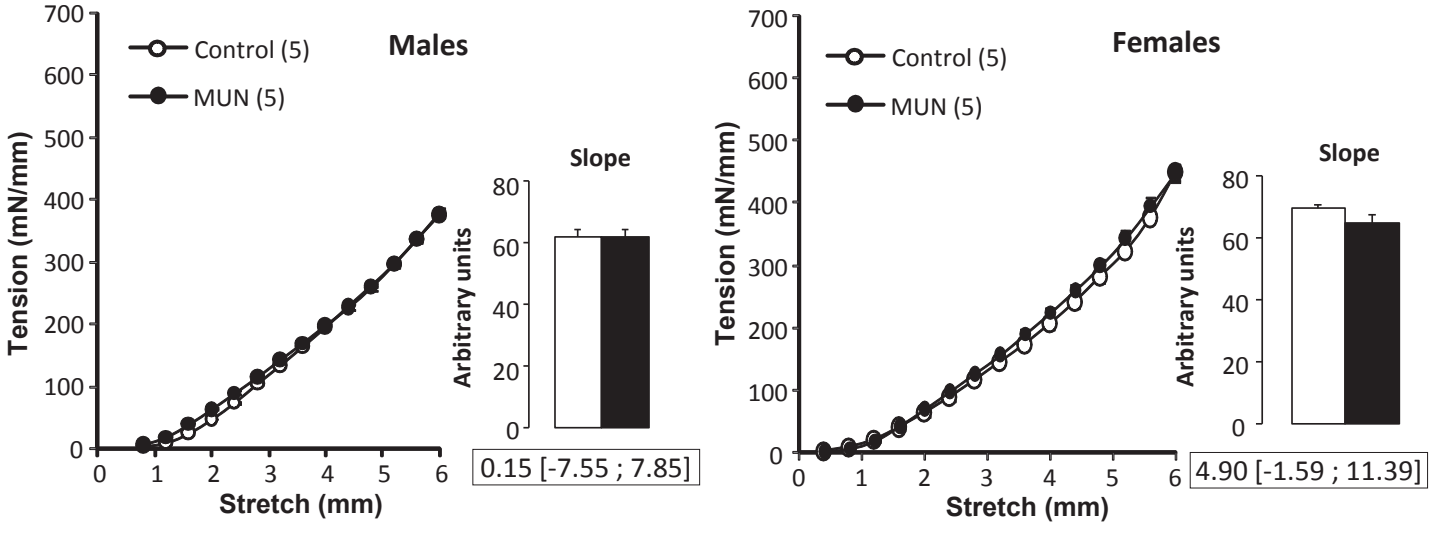

Figure 5

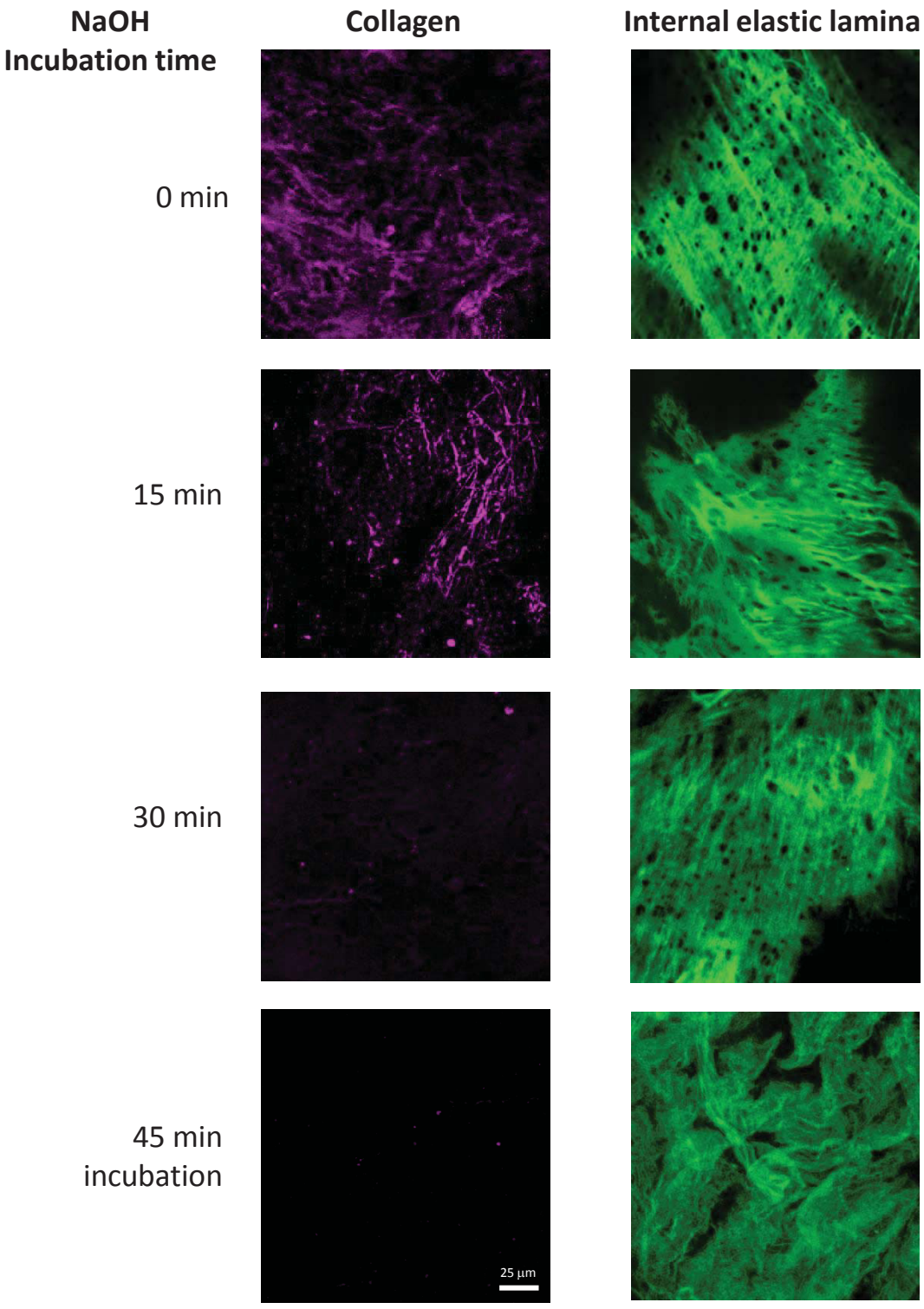
NaOH
Incubation time
Collagen
Internal elastic lamina
0 min
15 min
30 min
45 min
incubation
25 µm

Figure 6

A) Stretch-tension 21 days purified elastin

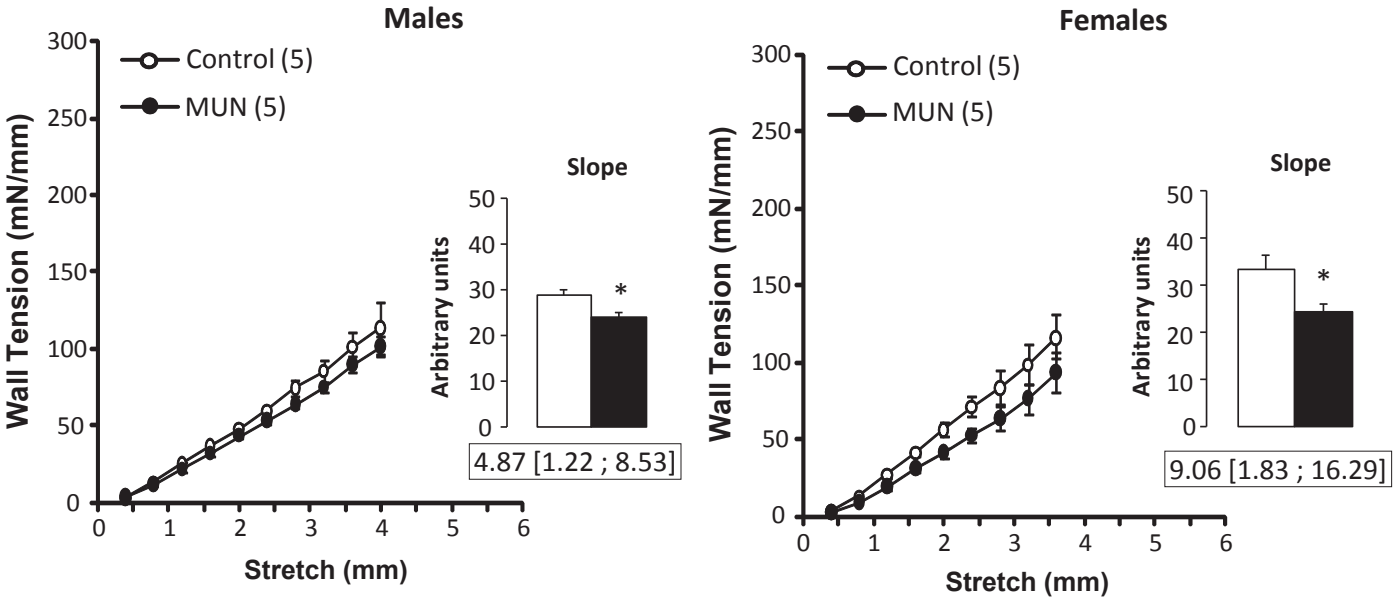

B) Stretch-tension 6 months purified elastin

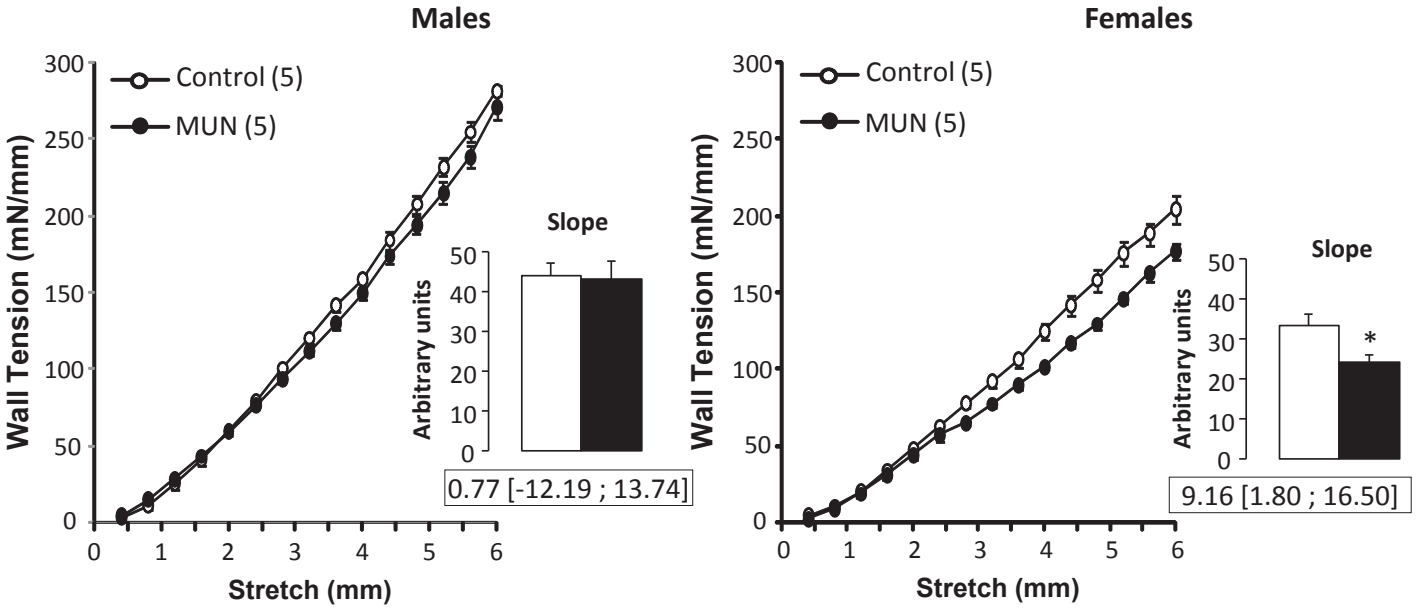

Figure 7

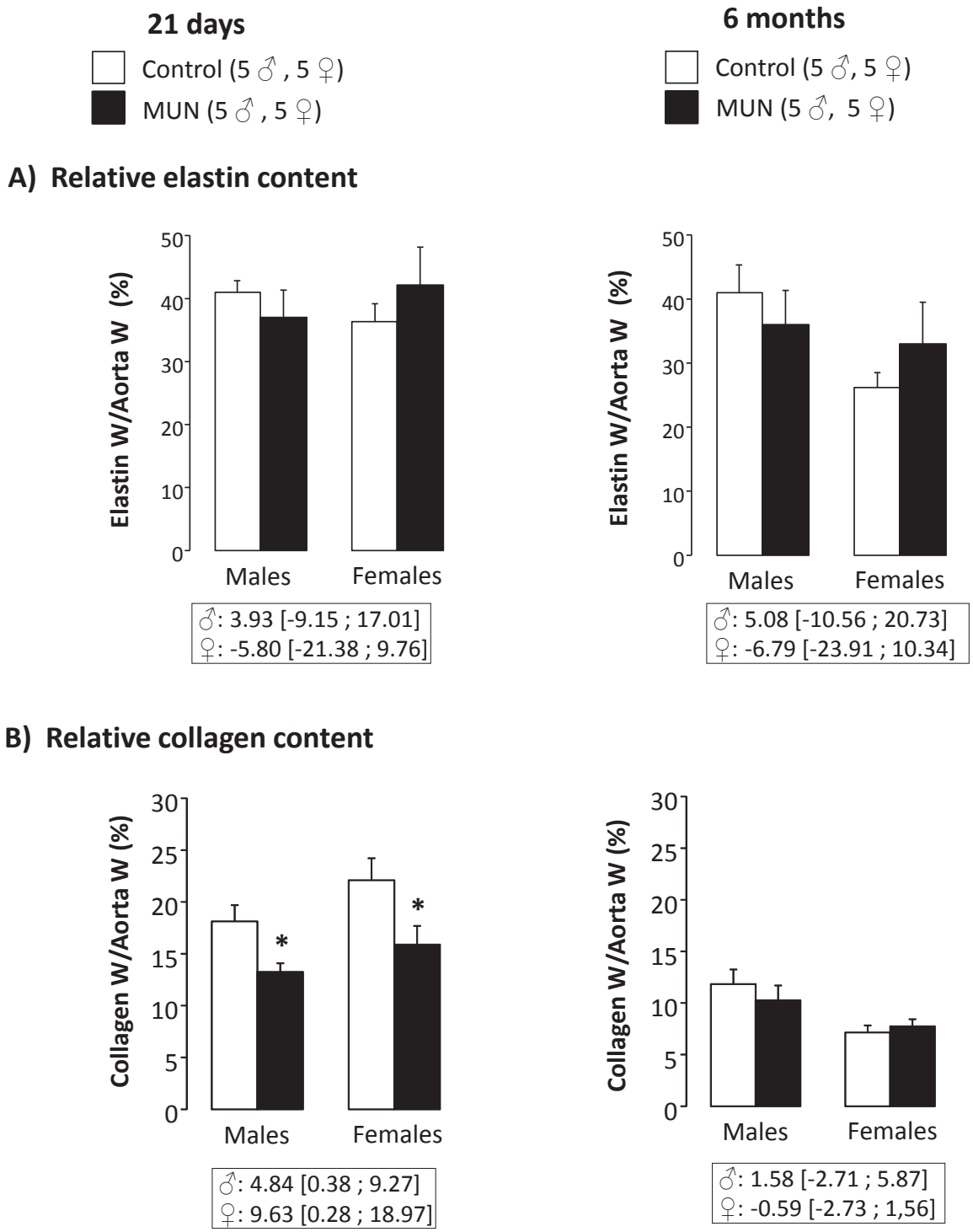
21 days
Control (5 ♂ , 5 ♀)
MUN (5 ♂ , 5 ♀)
6 months
Control (5 ♂, 5 ♀)
MUN (5 ♂, 5 ♀)
A) Relative elastin content
Elastin W/Aorta W (%)
50
40
30
20
10
0
Males
Females
♂: 3.93 [-9.15 ; 17.01]
♀: -5.80 [-21.38 ; 9.76]
Elastin W/Aorta W (%)
50
40
30
20
10
0
Males
Females
♂: 5.08 [-10.56 ; 20.73]
♀: -6.79 [-23.91 ; 10.34]
B) Relative collagen content
Collagen W/Aorta W (%)
30
25
20
15
10
5
0
*
*
Males
Females
♂: 4.84 [0.38 ; 9.27]
♀: 9.63 [0.28 ; 18.97]
Collagen W/Aorta W (%)
30
25
20
15
10
5
0
Males
Females
♂: 1.58 [-2.71 ; 5.87]
♀: -0.59 [-2.73 ; 1,56]

Figure 8

A) Internal elastic lamina organization in 21 day old rat aorta

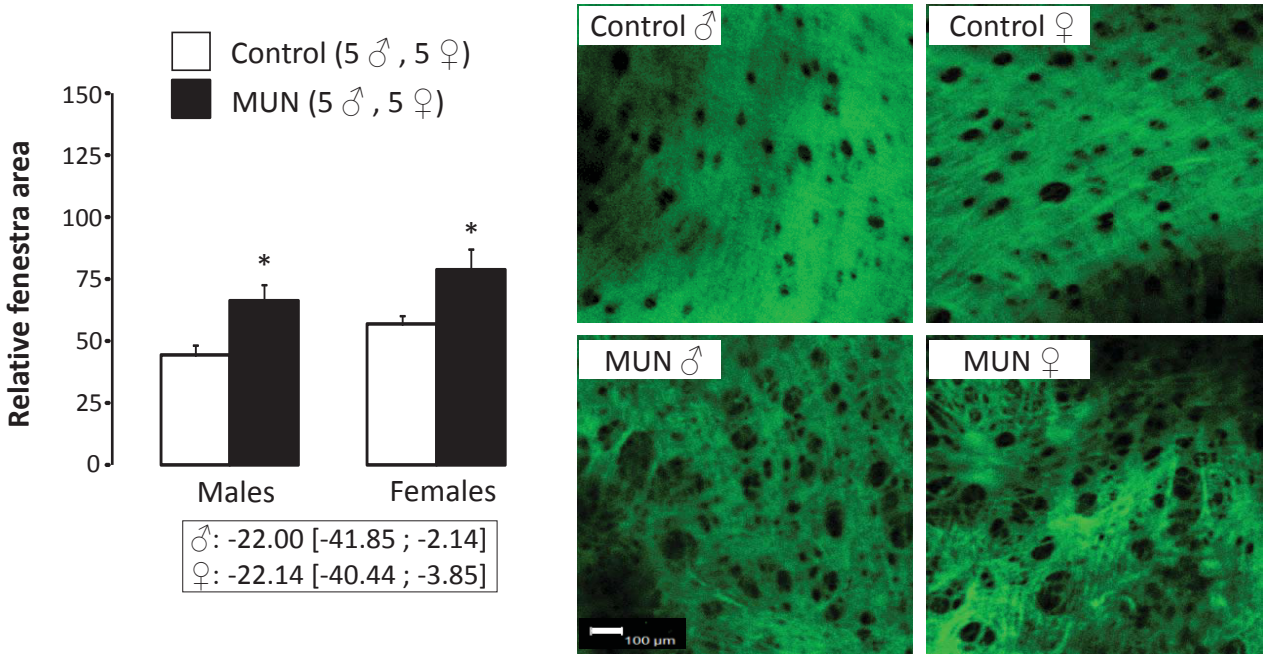

B) Internal elastic lamina organization in 6-month old rat aorta